

Article

Chemical Lasers Based on Polyatomic Reaction Dynamics: Research of Vibrational Excitation in a Reactive

José Daniel Sierra Murillo 

Departamento de Química, Universidad de La Rioja, 26006 Logroño, Spain; daniel.sierra@unirioja.es

Abstract: The research presented by the author investigates a polyatomic reaction occurring in the gas phase. This study employs the Quasi-Classical Trajectory (QCT) approach using the Wu–Schatz–Lendvay–Fang–Harding (WSLFH) potential energy surface (PES), recognized as one of the most reliable PES models for this type of analysis. The substantial sample size enables the derivation of detailed results that corroborate previous findings while also identifying potential objectives for future experimental work. The Gaussian Binning (GB) technique is utilized to more effectively highlight the variation in the total angular momentum (J') of the excited product molecule, HOD^* . A key aim of the study is to explore the reaction dynamics due to their importance in excitation and emission processes, which may contribute to the development of a chemical laser based on this reaction. Increasing the vibrational level, v , of one reactant, D_2 , significantly enhances the excitation of HOD^* and shifts the $P(J')$ distributions towards higher J' values, while also broadening the distribution. Although the current research focuses on a few initial conditions, the author plans to extend the study to encompass a wider range of initial conditions within the reaction chamber of this type of chemical laser.

Keywords: $\text{OH} + \text{D}_2$; gas phase reaction; Wu–Schatz–Lendvay–Fang–Harding potential energy surface; Quasi–Classical Trajectory; Vibrational and Rotational Gaussian Binning selections; chemical laser



Academic Editor: Jean-Christophe Pain

Received: 25 November 2024

Revised: 27 December 2024

Accepted: 5 January 2025

Published: 9 January 2025

Citation: Sierra Murillo, J.D. Chemical Lasers Based on Polyatomic Reaction Dynamics: Research of Vibrational Excitation in a Reactive. *Atoms* **2025**, *13*, 5. <https://doi.org/10.3390/atoms13010005>

Copyright: © 2025 by the author. Licensee MDPI, Basel, Switzerland. This article is an open access article distributed under the terms and conditions of the Creative Commons Attribution (CC BY) license (<https://creativecommons.org/licenses/by/4.0/>).

1. Introduction

The gas–phase reaction $\text{OH} + \text{D}_2 \rightarrow \text{HOD}^* + \text{D}$ is a fundamental system in tetratomic reaction dynamics, akin to the well-known benchmark reaction $\text{OH} + \text{H}_2$. Such reactions are instrumental in performing large-scale computational processes, including dynamic simulations, which are showcased in this study. These simulations enable a high-level contrast with past and future theoretical and experimental results, offering insights into the underlying mechanisms of these types of systems [1,2]. Notably, reactions like $\text{OH} + \text{H}_2$ serve as exemplary models for atom abstraction processes, where the OH radical abstracts a hydrogen atom (or deuterium in this case) from the D_2 molecule, forming the excited product molecule, HOD^* . This reaction mirrors the $\text{OH} + \text{H}_2$ system, in which the abstraction leads to the excited molecule HOH^* , commonly used as a benchmark for this type of reaction.

Although the current research lacks some experimental results necessary for a complete comparison, it presents a clear pathway for future experimental investigations aimed at obtaining these critical data. These findings are vital for expanding our understanding of this reaction system. In particular, the influence of initial vibrational and translational excitations on the reaction dynamics, as well as the effects of isotopic substitutions, has been a focus of previous experimental efforts. For example, studies have examined how

vibrational excitation influences the rate and product distribution in reactions of this type, providing a foundation for future work [3].

In the past, Alagia et al. conducted significant experimental work on the reaction $\text{OH} + \text{D}_2 \rightarrow \text{HOD} + \text{D}$, [4,5] where they were able to identify key aspects of the energy distribution but were unable to resolve the vibrational levels of HOD. Nevertheless, their findings demonstrated that approximately 64% of the total available energy was transferred into the internal energy of HOD [6]. These results were later confirmed by B.R. Strazisar et al. [6] who not only corroborated the energy distribution but also successfully resolved the vibrational states of the product molecule, HOD. In more recent studies, Liu et al. [7] and other research groups have continued to expand our understanding of this reaction, confirming and refining previous results while providing new insights into various characteristics of the reaction dynamics.

On the theoretical front, the development of potential energy surfaces (PES) has been essential in validating experimental results and providing insights into reaction mechanisms. The first theoretical approaches led to the creation of the pioneering WDSE (Walch–Dunning–Schatz–Elgersma) PES, [8] which successfully reproduced some of the experimental data obtained for reactions such as $\text{OH} + \text{D}_2$. Subsequent advancements in PES development include the OC (Ochoa–Clary) [9,10] and WSLFH (Wu–Schatz–Lendvay–Fang–Harding) [11] surfaces, which have proven to be highly effective in modeling this type of reaction. In 2010, Bowman et al. [12] reported on full-dimensional, electronically adiabatic potential energy surfaces for the ground state and excited state of OH_3 . More recent work has focused on Neural Network (NN) PES models, such as those developed by Chen et al. [13] which utilize machine learning techniques to predict energy surfaces with greater accuracy and efficiency. Despite the advances in NN PES, some challenges remain. For instance, previous work by the author [1,14] has identified a discontinuity in the transition state region of this NN PES [13], which may explain the inability to accurately capture energy distribution in half of the reactive trajectories. Or Quanli Ma et al., who note, according to their own words: “For the interaction of $\text{OH}(X^2\Pi)$ with H_2 , under the assumption of fixed OH and H_2 bond distances, we have determined two new sets of four-dimensional ab initio potential energy surfaces.” [15] In addition to NN PES, other non-analytical PES, such as the YZCL2 (Yang–Zhang–Collins–Lee) [16] and XXZ (C. Xiao, X. Xu, S. Liu, T. Wang, W. Dong, T. Yang, Z. Sun, D. Dai, D. H. Zhang and X. Yang) [17], have demonstrated their quality in describing reaction dynamics and energy transfer processes in related systems.

The methodology employed in this study, including Gaussian Binning (GB), [18–20] plays a crucial role in analyzing large data sets obtained from the simulations. GB methodology is particularly effective when dealing with very large samples, such as those used in this article, and is especially useful when analyzing vibro-rotational energy distributions through a two-step process: first, a Vibrational–GB (V–GB) selection followed by a Rotational–GB (R–GB) selection [1,14]. This approach ensures that the distributions are accurately represented, leading to more precise results.

Over the past few years, significant theoretical and experimental investigations have been conducted in the field of polyatomic reactions, particularly those related to systems like the one studied in this article [21–27]. These studies have furthered our understanding of the dynamics of such reactions and have provided valuable insights into the factors that influence energy transfer and product formation in these systems. Some recent contributions [28–31] in the field include studies on the influence of vibrational excitation on reaction dynamics, as well as investigations into the effects of isotopic substitution on product distribution. These works have been instrumental in expanding our knowledge of this important reaction system and have provided a solid foundation for future research.

In particular, the possibility of using reactions like $\text{OH} + \text{D}_2 \rightarrow \text{HOD} + \text{D}$ in chemical laser applications has been a subject of increasing interest. The development of chemical lasers based on reactions like this one could lead to advances in a variety of fields, including materials processing, spectroscopy, and fundamental research in molecular dynamics. The emitted wavelengths from such reactions could be extremely useful for manipulating physicochemical systems, particularly those that involve molecules that can be excited or dissociated under controlled conditions. The current study aims to further investigate this possibility and contribute to the development of a chemical laser based on the $\text{OH} + \text{D}_2$ reaction.

The contributions from recent studies in this area have significantly enhanced the understanding of the dynamics of this reaction system and have provided invaluable information for the design of future experimental and theoretical investigations. The author acknowledges and appreciates the important contributions made by these researchers, whose work has provided essential insights that have expanded the scope of his own research and will continue to inform future studies in the field.

The remainder article is organized as follows: Section 2 describes the computational method. Section 3 shows the results and discussion. Finally, Section 4 provides the concluding remarks.

2. Computational Method

$\text{OH} (v = 0; j = 2) + \text{D}_2 (v = 0, 1, 2, 3, 4; j = 2)$ for a collision energy of 0.28 eV are initial conditions studied in this article, although the author has planned to follow extending his research to vast samples of initial conditions that improve the knowledge about a possible chemical laser. Large samples of these initial conditions have been studied in this article (Table 1). They were calculated using QCT calculations and analyzed by means of GB methodology. Only WSLFH analytical PES was used, because of its good chemical–physical behavior and efficiency to obtain enough large samples of good results to analyze in a less time of calculus. Then, translational, vibrational, and rotational state distributions for HOD product molecules were analyzed by means of GB methodology. It is a very good method, as shown in the results obtained by the author in Refs. [1,14,19]. They had a great agreement with the experiments carried out with a high-resolution molecular beam [6,7]. GB methodology is better than the habitual histogram binning methodology, as shown in previous publications by the author.

Table 1. Summary of QCT calculated and QCT–GB selections for WSLFH PES. The meaning of the acronyms used in this table are also indicated throughout the article: TT (Total Trajectories), TRT (Total Reactive Trajectories), GRT (Good Reactive Trajectories), V–GB (first Vibrational–GB selection on GRT) and R–GB (second Rotational–GB selection on V–GB trajectories).

$v\text{D}_2$	TT	TRT	GRT	V–GB	R–GB
0	102,098,979	1,483,121	1,483,119	2267	224
1	55,000,000	2,315,774	2,314,719	2022	206
2	25,000,000	2,034,409	2,025,653	2188	216
3	14,691,407	1,705,064	1,678,727	1894	197
4	9,629,120	1,433,845	1,396,695	1289	146

2.1. Procedure to Generate Each Trajectory

As in preceding QCT–GB publications, [1,14,19] the author uses a similar strategy in the present article. Then, he gives a summary here. Between 100 M and 10 M trajectories were run for each of the initial conditions in reagents: $\text{OH} (v_{\text{OH}} = 0; j_{\text{OH}} = 2)$, and $\text{D}_2 (v_{\text{D}_2} = 0, 1, 2, 3, 4; j_{\text{D}_2} = 2)$. Total Trajectories (TT) calculated are started and stopped when

the separations between two molecules, in reactants (OH and D₂), and in products (HOD and D), are 10 bohr, with an integration time step of 10 au (0.24 fs) and the energy conservation is better than 1 in 1000. The product vibrational actions of HOD are determined at the end of each reactive trajectory using the Fourier Series method [32,33].

2.2. Analysis of Total Reactive Trajectories (TRT)

Like in the previous publications, the author considers Good Reactive Trajectories (GRT) those reactive trajectories that conserve the energy better than 1 in 1000 (Table 1).

To determine the vibrational actions corresponding to the HOD product molecule in each of the trajectories, the Fourier Series methodology [32,33] is used. Knowing the coordinates and momenta of said molecule at the end of each trajectory, and given their time dependency, they would be integrated for 1 ps using the corresponding classical equations of motion applied to an isolated system: in this case, the HOD molecule. That is, in the same manner as during the QCT calculations in the product area (HOD + D), but with removing the atom partner (D). From the coordinates and momenta developed as a function of the Fourier Series, the non-integer vibrational quantum numbers, N_k' ($k = 1(\text{HO}), 2(\text{HOD}), \text{and } 3(\text{OD})$), are calculated. These correspond to the classical actions of the product molecule HOD.

Expression used for vibrational energy, E_V' , of HOD product molecule is:

$$E_V' = \sum_k (N_k' + 1/2) \cdot h \cdot \nu_k'$$

where the sum extends to the three vibrational modes, N_k' ("real" values), and ν_k' are action and harmonic frequency of the k th vibrational mode, respectively.

For rotational energy, E_R' , of same HOD product molecule:

$$E_R' = 1/2 \cdot \langle \mathbf{fsj}' \mid I^{-1} \mid \mathbf{fsj}' \rangle + \text{Coriolis Coupling Term.}$$

where the bracket expression, $\langle \dots \mid \dots \mid \dots \rangle$, applies to the inner angular momentum (the module of vector \mathbf{fsj}' (\mathbf{fsj}') is a "real" value) and the inertial matrix (I) of HOD product molecule.

Finally, for translational energy, E_T' , between products (HOD and D):

$$E_T' = (p'_{\text{HOD,D}})^2 / 2 \cdot \mu_{\text{HOD,D}}$$

where $p'_{\text{HOD,D}}$ and $\mu_{\text{HOD,D}}$ are the linear momentum and the reduced mass, respectively, of the product system, HOD + D.

2.3. First Vibrational-GB (V-GB) Selection on GRT

QCT-GB analyses were completed as in some previous articles by the author [1,14,19]. A Gaussian statistical weight is given for each GRT, such that the closer the final non-integer vibrational actions of HOD, (N_1', N_2', N_3'), to integer values, ($\nu_{\text{HO}}', \nu_{\text{HOD}}', \nu_{\text{OD}}'$), defining this one the correspondent final vibrational state of HOD product molecule:

$$|N_1' - \nu_{\text{HO}}'| < \text{sqrt}(\ln(2)) \times 0.05 \approx 0.042.$$

$$|N_2' - \nu_{\text{HOD}}'| < \text{sqrt}(\ln(2)) \times 0.05 \approx 0.042.$$

$$|N_3' - \nu_{\text{OD}}'| < \text{sqrt}(\ln(2)) \times 0.05 \approx 0.042.$$

That is, that weight is a product of three narrow Gaussian functions, like the following expressions:

$$\exp[-(N_k' - v_k')^2 / \varepsilon^2], \quad k = 1(\text{HO}), 2(\text{HOD}), 3(\text{OD}).$$

With ε being a parameter kept at 0.05, its typical value. This method permits to apply Bohr quantization of HOD product vibration motions in a simple manner. Vibrational-state populations are then kept proportional to the sum of the Gaussian weights associated with the states [18,20].

V-GB selection requires about 1000 times more trajectories than the standard QCT approach, because this traditional methodology processes all trajectories without discriminating their different importance. For the GB methodology, each Gaussian has a full width at half maximum of ~ 0.1 , then is accountable for only 10% of the trajectories that actually contribute to the reactivity. In this case, HOD (N_1' , N_2' , N_3'), it is necessary three Gaussians, and their product does that the number of trajectories selected (V-GB) be three orders of magnitude less than the number of GRT.

2.4. Second Rotational-GB (R-GB) Selection on V-GB Trajectories

Another important information about the HOD product molecule is the rotational-state-specific distribution, $P(J')$, R-GB), where J' is the total angular momentum of that molecule in products. This new study was possible thanks to the improvement of the statistics here performed (Table 1).

fsj' , is obtained from the analysis of the rotational dynamics of each HOD product molecule of previously selected trajectories: V-GB trajectories. From the real number, fsj' , the nearest integer number to fsj' is the action (J') corresponding to the total angular momentum of the HOD product molecule. For this second GB selection, R-GB, only trajectories that verify the following condition are chosen:

$$|fsj' - J'| < 0.05.$$

The parameter (0.05) used in this second selection, R-GB, is less restrictive than the one used in the first selection, V-GB. Therefore, the number of trajectories selected (R-GB) decreases to a lesser extent than for the first selection (V-GB). This R-GB selection just produces a decrease of one order of magnitude on V-GB paths (Table 1).

3. Results and Discussions

3.1. Energies Disposal in Products

Energies disposal in products, calculated on WSLFH PES with three statistics (GRT, V-GB, and R-GB) and five initial conditions for the reactive components (OH + D₂ ($vD_2 = 0, 1, 2, 3, 4; jD_2 = 2$)), are presented in Table 2.

The increase of the vibrational excitation of D₂ ($vD_2 \rightarrow 0, 1, 2, 3, 4$) causes variations and redistributions of energies in products (HOD + D) (Table 2). Particularly, it produces a light augment of the vibrational fraction (51–61% to 69–68%) but a significant decrease of the translational fraction (41–33% to 18–20%) and a middle augment for the rotational fraction (8–6% to 14–13%). Nevertheless, the increase in the initial conditions of vD_2 produces a redistribution of energies disposal in products in another sense, helping a significant increase of vibrational (11–13 to 39–38 kcal·mol⁻¹) and rotational (2–1 to 8–7 kcal·mol⁻¹) levels but a less one in the translational energy (9–7 to 10–11 kcal·mol⁻¹). Subsequently, it produces an increase of the inner energy (vibrational and rotational levels), as shown in the next sections.

Table 2. Energies disposal in products ($\text{kcal}\cdot\text{mol}^{-1}$) for GRT, V-GB, and R-GB trajectories when $\nu\text{D}_2 = 0, 1, 2, 3, 4$. All energies are expressed in terms of average and fraction ones, respectively, for vibrational (V), translational (T) and rotational (R) kinds.

	$\langle E_V \rangle$ and (f_V')	$\langle E_T \rangle$ and (f_T')	$\langle E_R \rangle$ and (f_R')
GRT (0)	10.97 (50.74%)	8.95 (41.38%)	1.70 (7.88%)
V-GB (0)	12.64 (58.11%)	7.63 (35.08%)	1.48 (6.80%)
R-GB (0)	13.36 (61.27%)	7.21 (33.08%)	1.23 (5.66%)
(1)	19.13 (62.29%)	8.35 (27.18%)	3.24 (10.53%)
	17.71 (57.92%)	9.57 (31.30%)	3.29 (10.77%)
	18.38 (60.10%)	9.26 (30.29%)	2.94 (9.61%)
(2)	25.43 (64.44%)	8.97 (22.72%)	5.07 (12.84%)
	25.37 (64.14%)	9.32 (23.56%)	4.86 (12.30%)
	25.60 (64.66%)	9.64 (24.36%)	4.35 (10.99%)
(3)	31.57 (66.02%)	9.66 (20.20%)	6.59 (13.78%)
	31.72 (66.09%)	9.89 (20.61%)	6.38 (13.30%)
	31.53 (65.46%)	10.11 (20.99%)	6.53 (13.55%)
(4)	38.60 (68.84%)	9.84 (17.55%)	7.64 (13.62%)
	36.96 (65.96%)	11.40 (20.35%)	7.67 (13.69%)
	37.95 (67.63%)	10.98 (19.57%)	7.19 (12.81%)

3.2. $P(J')$ vs. $(\nu_{\text{HO}}', \nu_{\text{HOD}}', \nu_{\text{OD}}')$ on R-GB Trajectories Selected

The rotational angular momentum distributions, $P(J')$, of the HOD product molecule, after the second selection, R-GB, is shown at Figure 1.

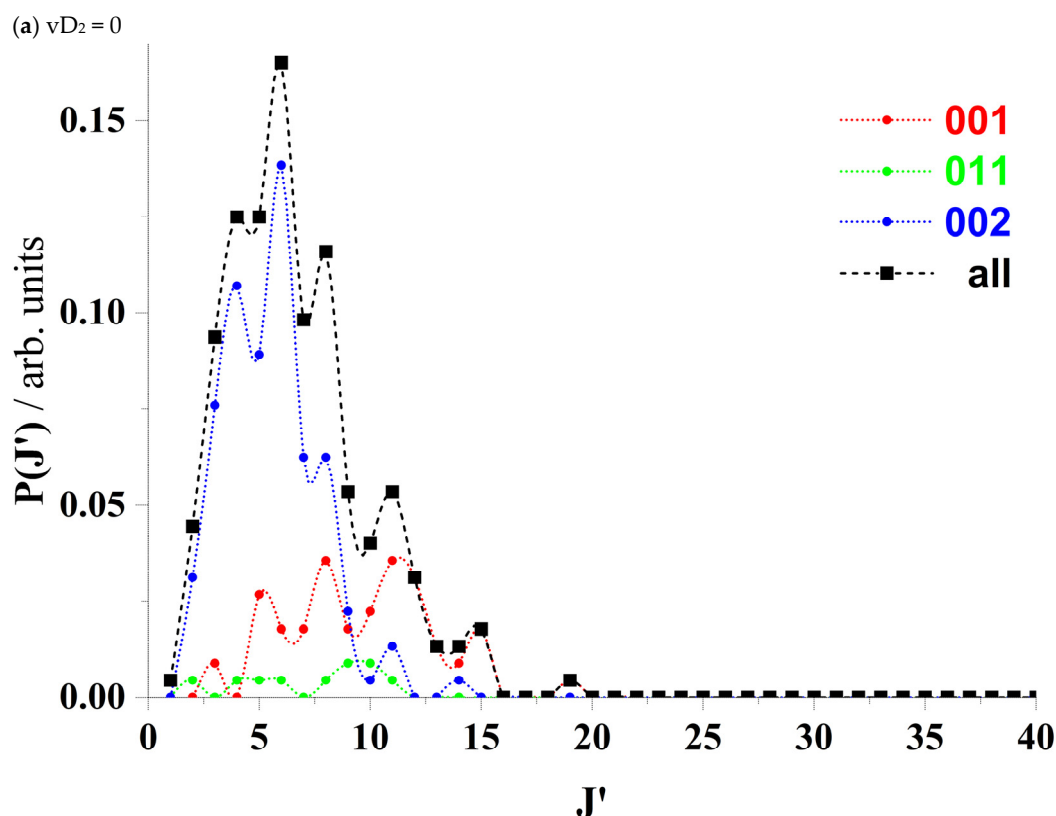
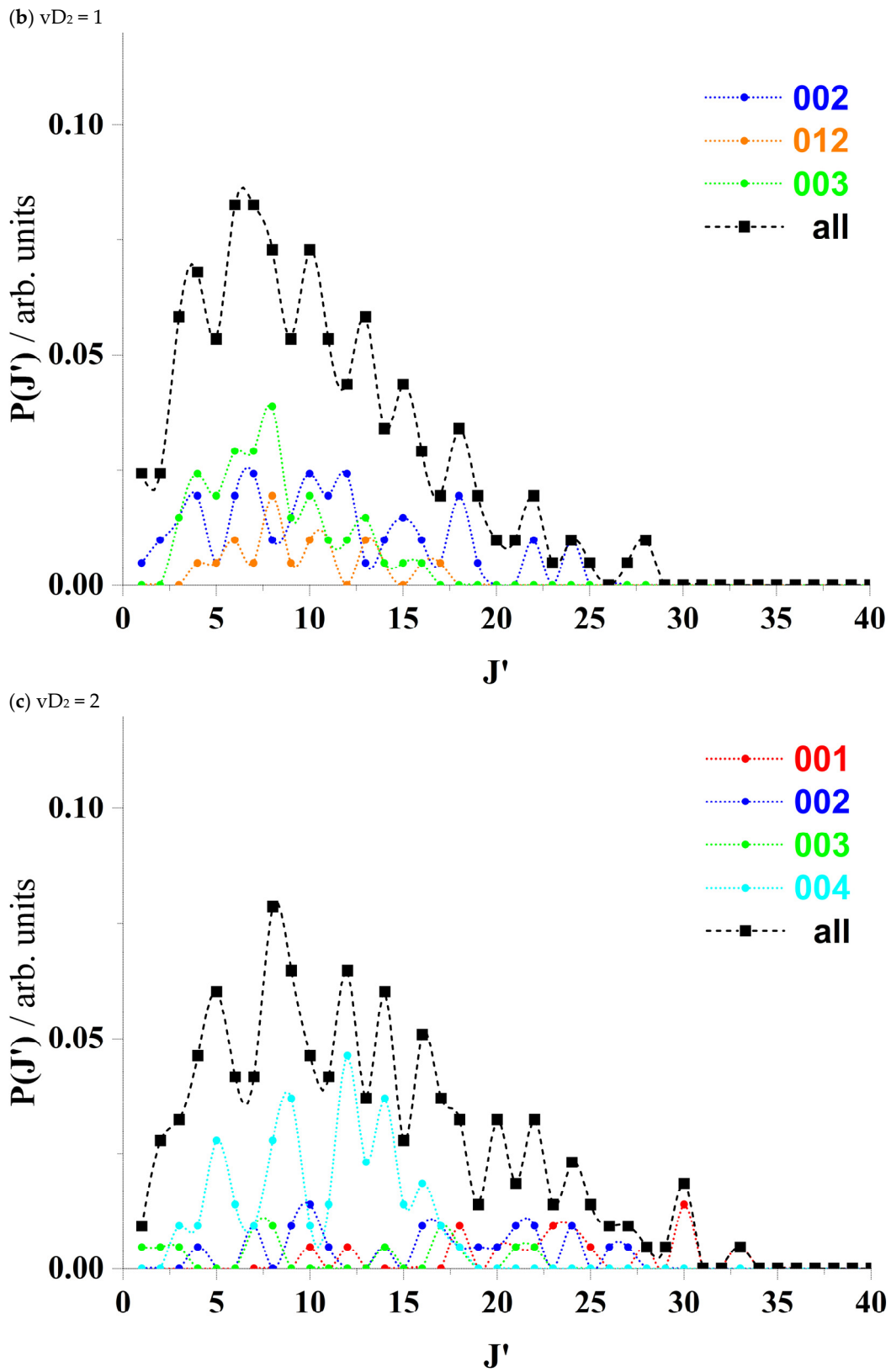


Figure 1. Cont.



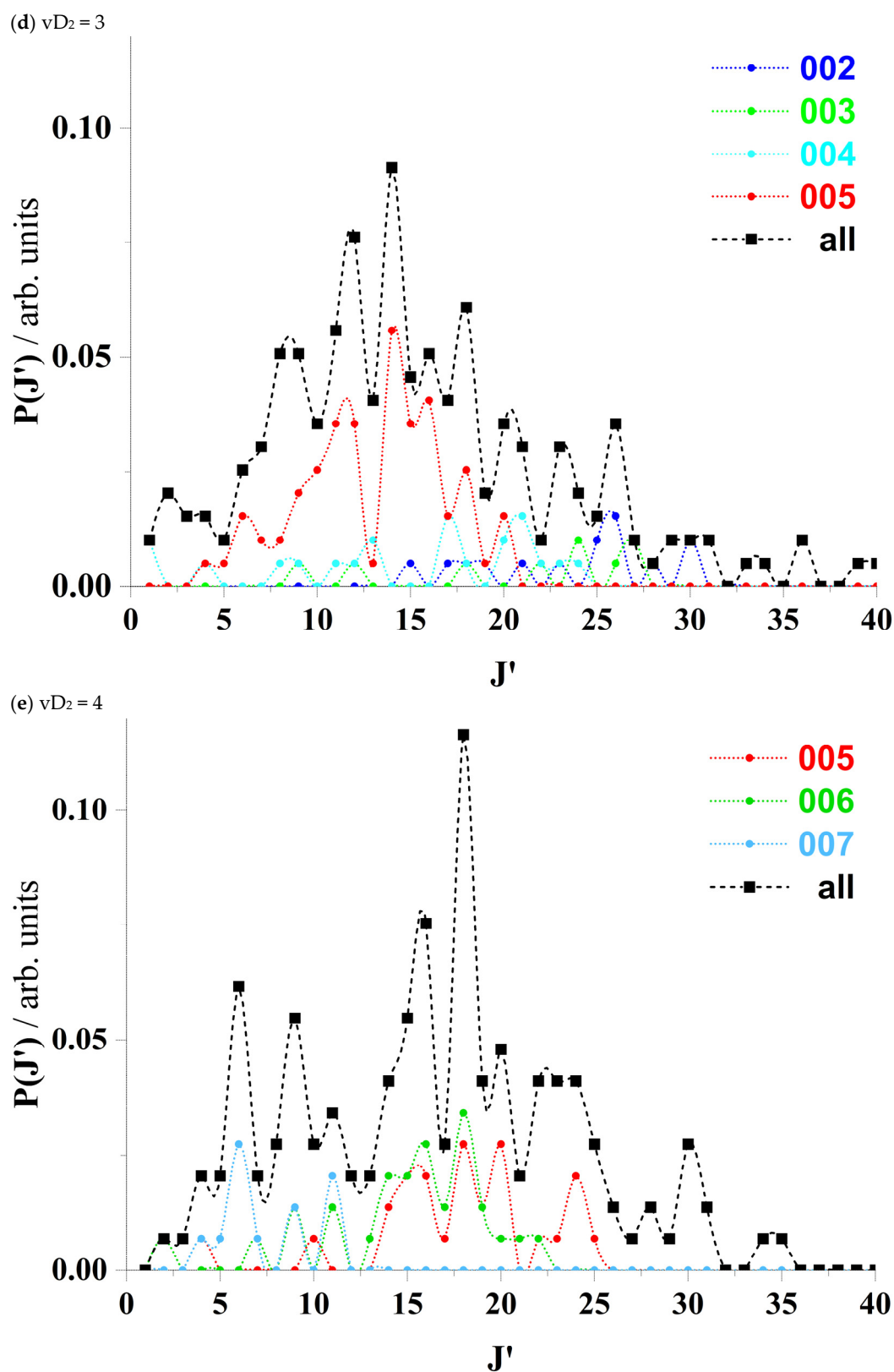


Figure 1. (a–e). $P(J')$ after a second selection, R–GB. $P(J')$ distributions are divided in 40 bin's ($J' = 1, \dots, 40$) and normalized to the unity the sum of the set of all probability distributions. The $P(J')$ (all) distribution is the sum of all possible distributions, $P(J')(v_{HO'}, v_{HOD'}, v_{OD'})$.

Figures below correspond to visualizations of some of the GB analyses (after V–GB and R–GB selections) of QCT calculations executed for the following initial conditions OH + D₂($v_{D_2} = 0$ (a), 1(b), 2(c), 3(d), 4(e)) on WSLFH PES.

It is important to remark that, according to the first V–GB selection, ($v_{HO'}$, $v_{HOD'}$, $v_{OD'}$), and the second selection, R–GB, a variable predilection for odd or even J' is detected. (Figure 1) The author believes it is important to remember that an analogous behavior is shown in another triatomic molecule utilized in the gas laser of CO_2 [34].

Global distributions (all) for the initial conditions considered in this research ($OH + D_2$ ($v_{D_2} = 0, 1, 2, 3, 4$)) are qualitatively similar in their oscillating behaviours. Nevertheless, quantifiable differences are shown for global (all) and specific distributions, $P(J')$. The author considers that it could be interesting to carry out experimental measurements to compare with the results of this paper. Furthermore, an increase of $v_{D_2} = 0, 1, 2, 3, 4$ provokes a considerable increase of vibrational levels in HOD product and a displacement of the distributions, $P(J')$, towards very higher values of J' but a greater dispersion of said distributions. This substantial dispersion could be due to the isotropic character induced by the increase of “ v_{D_2} ” in the reaction studied, $OH + D_2$ ($v_{D_2}; j = 2$) \rightarrow HOD + D, and then, in the HOD product molecule.

3.3. Discussion About V–GB and R–GB Selections in a Chemical Laser

The author would like to finish by saying that the dynamics of gas phase reactions like the present one ($OH + D_2 \rightarrow HOD^* + D$) can be of great interest for present and future gas/chemical lasers based in water vapor semi-deuterated, HOD^* . Then, the interest and importance of theoretical and experimental research. The processes of excitation and emission of the products of the aforementioned reactions could be studied by means of laser prototypes based on chemical reactions in the gas phase and adequately controlled to obtain behaviors based on the above theoretical investigations. The author proposes a constructive interaction between the theory used by him and experimentation in the form of laser prototypes, so that it produces a significant advance in the knowledge of the dynamics of the investigated systems related to the excitation and emission processes by one of the reaction products produced in the reaction camera of a possible chemical laser [35].

4. Summary and Conclusions

This work provides QCT calculations and GB analysis for the reaction above presented and the following initial conditions: OH ($v_{OH} = 0; j_{OH} = 2$) and D_2 ($v_{D_2} = 0, 1, 2, 3, 4; j_{D_2} = 2$).

Energies disposal in products ($HOD + D$) were calculated for large and good samples of simulated trajectories: GRT and trajectories obtained after both selections, V–GB and R–GB. It was shown that the increase of v_{D_2} induces changes in energies disposal in products. Remember that in previous articles, [1,14,19] it was shown that improvements in the statistics yields results that are good to those obtained under similar experimental conditions. This conclusion inspires the author with confidence in a possible coincidence with future experiments based in this theoretical research studied in the present article.

Depending on the result of the first selection, V–GB ($v_{HO'}$, $v_{HOD'}$, $v_{OD'}$), and given the asymmetry of the product molecule, HOD, when the second selection, R–GB, is realized, a variable predilection of even or odd values for the total angular momentum, J' , becomes apparent. Moreover, it is observed that an increase of $v_{D_2} = 0, 1, 2, 3, 4$ induces an increase of vibrational levels in HOD product and a displacement of the distributions, $P(J')$, towards very higher values of J' , but a greater dispersion of said distribution. This effect could be due to the isotropic behavior induced by the increase of “ v_{D_2} ” in the reaction studied, $OH + D_2$ ($v_{D_2}; j = 2$) \rightarrow HOD + D, and then, in the HOD product molecule.

It is important to recall an analogous behavior in the CO_2 triatomic molecule employed in this gas laser.

Funding: This research received no external funding.

Data Availability Statement: The author may share his data, calculated and analyzed on Beronia, on the condition that the person/s requesting them “certify” that they will not use them for profit and/or for their scientific benefit.

Acknowledgments: For this work, the author used a cluster named Beronia (beronia.unirioja.es), in University of La Rioja, which is supported by FEDER-MINECO grant number UNLR-094E-2C-225.

Conflicts of Interest: The authors declare no conflict of interest.

References

1. Sierra-Murillo, J.D. Vibrational and Rotational Gaussian Binning selections on QCT calculations for the $\text{OH} + \text{D}_2 \rightarrow \text{HOD}(\nu_{\text{HO}'}, \nu_{\text{HOD}'}, \nu_{\text{OD}'}, J') + \text{D}$ reaction. *Chem. Phys.* **2021**, *551*, 111351. [[CrossRef](#)]
2. Sierra-Murillo, J.D.; Martínez, R.; Hernando, J.; González, M. The $\text{OH} + \text{D}_2 \rightarrow \text{HOD} + \text{D}$ angle-velocity distribution: Quasi-classical trajectory calculations on the YZCL2 and WSLFH potential energy surfaces and comparison with experiments at $E_T = 0.28$ eV. *Phys. Chem. Chem. Phys.* **2009**, *11*, 11520. [[CrossRef](#)] [[PubMed](#)]
3. Smith, I.W.M.; Crim, F.F. The chemical kinetics and dynamics of the prototypical reaction: $\text{OH} + \text{H}_2 \rightarrow \text{H}_2\text{O} + \text{H}$. *Phys. Chem. Chem. Phys.* **2002**, *4*, 3543. [[CrossRef](#)]
4. Alagia, M.; Balucani, N.; Casavecchia, P.; Stranges, D.; Volpi, G.G. Crossed beam studies of four-atom reactions: The dynamics of $\text{OH} + \text{CO}$. *J. Chem. Phys.* **1993**, *98*, 8341. [[CrossRef](#)]
5. Alagia, M.; Balucani, N.; Casavecchia, P.; Stranger, D.; Volpi, G.G.; Clary, D.C.; Kliesch, A.; Werner, H.J. The dynamics of the reaction $\text{OH} + \text{D}_2 \rightarrow \text{HOD} + \text{D}$: Crossed beam experiments and quantum mechanical scattering calculations on ab initio potential energy surfaces. *Chem. Phys.* **1996**, *207*, 389. [[CrossRef](#)]
6. Strazisar, B.R.; Lin, C.; Davis, H.F. Mode-Specific Energy Disposal in the Four-Atom Reaction $\text{OH} + \text{D}_2 \rightarrow \text{HOD} + \text{D}$. *Science* **2000**, *290*, 958. [[CrossRef](#)]
7. Liu, S.; Xiao, C.; Wang, T.; Chen, J.; Yang, T.; Xu, X.; Zhang, D.H.; Yang, X. The dynamics of the $\text{D}_2 + \text{OH} \rightarrow \text{HOD} + \text{D}$ reaction: A combined theoretical and experimental study. *Faraday Discuss* **2012**, *157*, 101. [[CrossRef](#)]
8. Schatz, G.C.; Elgersma, H. A quasi-classical trajectory study of product vibrational distributions in the $\text{OH} + \text{H}_2 \rightarrow \text{H}_2\text{O} + \text{H}$ reaction. *Chem. Phys. Lett.* **1980**, *73*, 21. [[CrossRef](#)]
9. de Aspuru, G.O.; Clary, D.C. New Potential Energy Function for Four-Atom Reactions. Application to $\text{OH} + \text{H}_2$. *J. Phys. Chem. A* **1998**, *102*, 9631. [[CrossRef](#)]
10. Pogrebnya, S.K.; Palma, J.; Clary, D.C.; Echave, J. Quantum scattering and quasi-classical trajectory calculations for the $\text{H}_2 + \text{OH} \rightleftharpoons \text{H}_2\text{O} + \text{H}$ reaction on a new potential surface. *Phys. Chem. Chem. Phys.* **2000**, *2*, 693. [[CrossRef](#)]
11. Wu, G.; Schatz, G.C.; Lendvay, G.; Fang, D.-C.; Harding, L.B. A new potential surface and quasiclassical trajectory study of $\text{H} + \text{H}_2\text{O} \rightarrow \text{OH} + \text{H}_2$. *J. Chem. Phys.* **2000**, *113*, 3150, Erratum in *J. Chem. Phys.* **2000**, *113*, 7712. [[CrossRef](#)]
12. Fu, B.; Kamarchik, E.; Bowman, J.M. Quasiclassical trajectory study of the postquenching dynamics of $\text{OH} \text{A}^2\Sigma^+$ by H_2/D_2 on a global potential energy surface. *J. Chem. Phys.* **2010**, *133*, 164306. [[PubMed](#)]
13. Chen, J.; Xu, X.; Xu, X.; Zhang, D.H. A global potential energy surface for the $\text{H}_2 + \text{OH} \leftrightarrow \text{H}_2\text{O} + \text{H}$ reaction using neural networks. *J. Chem. Phys.* **2013**, *138*, 154301. [[CrossRef](#)]
14. Sierra-Murillo, J.D. High power laser from $\text{OH} + \text{D}_2 \rightarrow \text{HOD}(\nu_{\text{HO}'}, \nu_{\text{HOD}'}, \nu_{\text{OD}'}, J') + \text{D}$ reaction. In *Proceedings of the XXII International Symposium on High Power Laser Systems and Applications, Frascati, Italy, 9–12 October 2018*; Di Lazzaro, P., Ed.; SPIEDigitalLibrary.org: Bellingham, WA USA, 2019; Volume 11042, p. 1104209. [[CrossRef](#)]
15. Ma, Q.; Kłos, J.; Alexander, M.H.; van der Avoird, A.; Dagdigian, P.J. The interaction of $\text{OH} (\text{X}^2\Pi)$ with H_2 : *Ab initio* potential energy surfaces and bound states. *J. Chem. Phys.* **2014**, *141*, 174309. [[CrossRef](#)]
16. Yang, M.; Zhang, D.H.; Collins, M.A.; Lee, S.-Y. *Ab initio* potential-energy surfaces for the reactions. $\text{OH} + \text{H}_2 \rightarrow \text{H}_2\text{O} + \text{H}$. *J. Chem. Phys.* **2001**, *115*, 174. [[CrossRef](#)]
17. Xiao, C.; Xu, X.; Liu, S.; Wang, T.; Dong, W.; Yang, T.; Sun, Z.; Dai, D.; Zhang, D.H.; Yang, X. Experimental and Theoretical Differential Cross Sections for a Four-Atom Reaction: $\text{HD} + \text{OH} \rightarrow \text{H}_2\text{O} + \text{D}$. *Science* **2011**, *333*, 440. [[CrossRef](#)] [[PubMed](#)]
18. Bonnet, L.; Rayez, J.-C. Quasiclassical trajectory method for molecular scattering processes: Necessity of a weighted binning approach. *Chem. Phys. Lett.* **1997**, *277*, 183. [[CrossRef](#)]
19. Sierra-Murillo, J.D.; Bonnet, L.; Gonzalez, M. Quasi-Classical Trajectory–Gaussian Binning Study of the $\text{OH} + \text{D}_2 \rightarrow \text{HOD}(\nu_1', \nu_2', \nu_3') + \text{D}$ Angle–Velocity and Vibrational Distributions at a Collision Energy of 0.28 eV. *J. Phys. Chem. A* **2011**, *115*, 7413. [[CrossRef](#)]
20. Bonnet, L.; Larrégaray, P.; Arbelo-González, W.; de Castro-Vitores, M. Normalization of the Gaussian binning trajectory method for indirect reactions. *Comp. Theor. Chem.* **2012**, *990*, 30. [[CrossRef](#)]

21. Dagdigian, P.J. Collisional excitation of deuterated hydroxyl (OD) by molecular hydrogen. *Mon. Not. R. Astron. Soc.* **2021**, *505*, 1987. [[CrossRef](#)]
22. Huang, J.; Chen, J.; Liu, S.; Zhang, D.H. Time-dependent wave packet dynamics calculations of cross sections for ultracold four-atom reactions. *J. Phys. Chem. Lett.* **2020**, *11*, 8560. [[CrossRef](#)]
23. Malbon, C.L.; Zhao, B.; Guo, H.; Yarkony, D.R. On the nonadiabatic collisional quenching of OH (A) by H₂: A four coupled quasi-diabatic state description. *Phys. Chem. Chem. Phys.* **2020**, *22*, 13516. [[CrossRef](#)]
24. Klos, J.; Dagdigian, P.J.; Alexander, M.H.; Faure, A.; Lique, F. The excitation of OH by H₂ revisited—II. Hyperfine resolved rate coefficients. *Mon. Not. R. Astron. Soc.* **2020**, *493*, 3491. [[CrossRef](#)]
25. Shu, Y.; Kryven, J.; de Oliveira-Filho, A.G.S.; Zhang, L.; Song, G.-L.; Li, S.L.; Meana-Pañeda, R.; Fu, B.; Bowman, J.M.; Truhlar, D.G. Direct diabaticization and analytic representation of coupled potential energy surfaces and couplings for the reactive quenching of the excited ²Σ⁺ state of OH by molecular hydrogen. *J. Chem. Phys.* **2019**, *151*, 104311. [[CrossRef](#)] [[PubMed](#)]
26. Klos, J.; Ma, Q.; Dagdigian, P.J.; Alexander, M.H.; Faure, A.; Lique, F. The excitation of OH by H₂ revisited—I: Fine-structure resolved rate coefficients. *Mon. Not. R. Astron. Soc.* **2017**, *471*, 4249. [[CrossRef](#)]
27. Schewe, H.C.; Ma, Q.; Vanhaecke, N.; Wang, X.; Klos, J.; Alexander, M.H.; van de Meerakker, S.Y.T.; Meijer, G.; van der Avoird, A.; Dagdigian, P.J. Rotationally inelastic scattering of OH by molecular hydrogen: Theory and experiment. *J. Chem. Phys.* **2015**, *142*, 204310. [[CrossRef](#)]
28. Czakó, G.; Gruber, B.; Papp, D.; Tajti, V.; Tasi, D.A.; Yin, C. First-principles mode-specific reaction dynamics. *Phys. Chem. Chem. Phys.* **2024**, *26*, 15818. [[CrossRef](#)]
29. Braunstein, M.; Bonnet, L. A quasi-classical study in a quantum spirit of mode specificity of the H+ HOD abstraction reaction. *Phys. Chem. Chem. Phys.* **2024**, *26*, 26084. [[CrossRef](#)] [[PubMed](#)]
30. Sierra-Murillo, J.D. Chemical laser based on polyatomic chemical reaction dynamics. In Proceedings of the SPIE 12347, XXIII International Symposium on High Power Laser Systems and Applications, Prague, Czech Republic, 13–16 June 2022; SPIEDigital-Library.org: Bellingham, WA USA, 2022; Volume 12347, p. 1234707. [[CrossRef](#)]
31. Rawlins, K.; Mookerjee, B. Investigating the OH–H₂ relation in diffuse Galactic clouds. *Mon. Not. R. Astron. Soc.* **2023**, *523*, 4593.
32. Schatz, G.C. A program for determining primitive semiclassical eigenvalues for vibrating/rotating nonlinear triatomic molecules. *Comput. Phys. Commun.* **1988**, *51*, 135. [[CrossRef](#)]
33. GSchatz, C.; Horst, M.T.; Takayanagi, T. *Modern Methods for Multidimensional Dynamics Computations in Chemistry*; Thompson, D.L., Ed.; World Scientific: Singapore, 1998; pp. 1–33.
34. Svelto, O. *Principles of Lasers*, 5th ed.; Springer: Berlin/Heidelberg, Germany, 2010; p. 447.
35. Salman (Zamik) Rosenwaks. Reflections on the history of chemical lasers research. In Proceedings of the XXI International Symposium on High Power Laser Systems and Applications 2016, Gmunden, Austria, 5–9 September 2016; SPIE Digital Library: Bellingham, WA, USA, 2017; Volume 10254, p. 102540G. [[CrossRef](#)]

Disclaimer/Publisher’s Note: The statements, opinions and data contained in all publications are solely those of the individual author(s) and contributor(s) and not of MDPI and/or the editor(s). MDPI and/or the editor(s) disclaim responsibility for any injury to people or property resulting from any ideas, methods, instructions or products referred to in the content.